SHORT COMMUNICATION

Focused library of phenyl-fused macrocyclic amidinoureas as antifungal agents
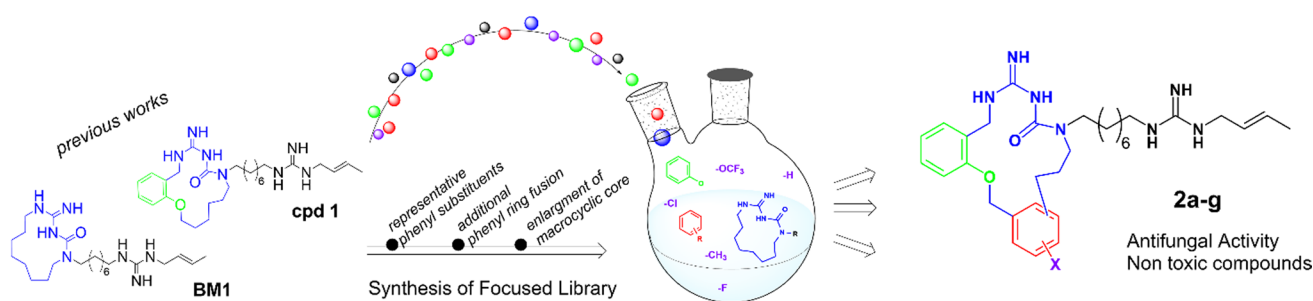
Lorenzo J. I. Balestri[1] · **Ilaria D'Agostino**[1] · **Enrico Rango**[1] · **Chiara Vagaggini**[1] · **Rosalba Marchitiello**[2] ·
Melinda Mariotti[2] · **Alexandru Casian**[1] · **Davide Deodato**[1] · **Giuseppina I. Truglio**[1] · **Francesco Orofino**[1] ·
Maurizio Sanguinetti[2,3] · **Francesca Bugli**[2,3] · **Lorenzo Botta**[4,5] · **Elena Dreassi**[1]

Abstract

The rise of antimicrobial-resistant phenotypes and the spread of the global pandemic of COVID-19 are worsening the outcomes of hospitalized patients for invasive fungal infections. Among them, candidiases are seriously worrying, especially since the currently available drug armamentarium is extremely limited. We recently reported a new class of macrocyclic amidinoureas bearing a guanidino tail as promising antifungal agents. Herein, we present the design and synthesis of a focused library of seven derivatives of macrocyclic amidinoureas, bearing a second phenyl ring fused with the core. Biological activity evaluation shows an interesting antifungal profile for some compounds, resulting to be active on a large panel of *Candida* spp. and *C. neoformans*. PAMPA experiments for representative compounds of the series revealed a low passive diffusion, suggesting a membrane-based mechanism of action or the involvement of active transport systems. Also, compounds were found not toxic at high concentrations, as assessed through MTT assays.

Graphical abstract

Lorenzo J.I. Balestri and Ilaria D'Agostino have contributed equally to the work.

This work is dedicated to Prof. Maurizio Botta, whose hard work and strong devotion to medicinal chemistry research were and still continue to be a source of inspiration for students and researchers.

✉ Elena Dreassi
elena.dreassi@unisi.it

Extended author information available on the last page of the article

Introduction

Nowadays, the burden of systemic fungal infections is threatening public health. Numbers speak for themselves: annually, more than 150 million people are estimated to suffer from fungal diseases, resulting in a considerable negative impact on their life [1]. Invasive fungal infections (IFIs) are among the most common nosocomial infections, [2] killing up to 1.5 million people each year [3]. IFIs are related to severe illness and high mortality [4–6] in patients with immunocompromised conditions. Moreover, the global
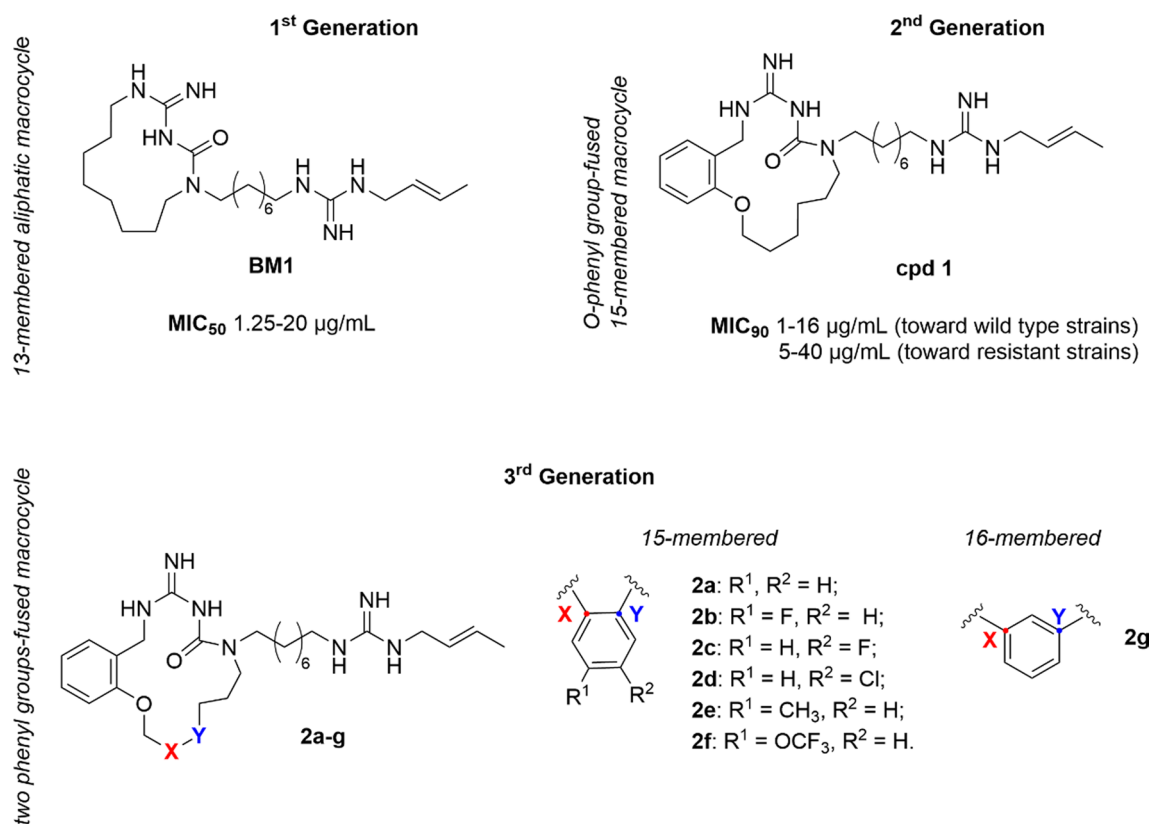
Fig. 1 Structure of **BM1**, compound **1**, and derivatives **2a–g** described in this paper with MIC ranges against *Candida* spp. strains

emergency caused by SARS-CoV-2 worsened the scenario, leading affected people to intubation, mechanical ventilation, and long-term hospitalization that increase the susceptibility to the development of fungal infections [7–9]

Candida species are responsible for nearly half of IFIs [10, 11]. The most predominant pathogenic strain in bloodstream infections is *C. albicans*. However, recently, diseases caused by non-*albicans Candida* (NAC) species are increasing in concern [12]. Currently available treatments are mainly represented by azoles, the only orally available class in clinics. Unfortunately, *C. krusei*, *C. auris*, and *C. glabrata,* belonging to NAC species, are characterized by a low intrinsic susceptibility to these antifungals and are highly prone to develop resistomes [10]. Moreover, *C. glabrata* displayed a high capacity to form biofilms on artificial devices and epithelial surfaces, leading to a reduction in the drug absorption and consequent decreases in the treatment efficacy [13–15].

Besides *Candida* species, *Cryptococcus neoformans* is highly invasive in humans, causing life-threatening meningitis [16], especially in resource-limited regions where treatments of choice based on amphotericin B and 5-flucytosine are not available since too expensive [17].

However, the clinically available antifungal arsenal is still limited to old drug classes, and the more recently developed, the echinocandins, can be traced back to the early 2000s [13, 15, 17]. Only one drug candidate, Fosmanogepix, a broad-spectrum antifungal agent, is endowed with an innovative mode of action (MoA), but it is still in clinical trials [18]. Furthermore, no vaccine has still received the food and drug administration (FDA) approval to date. Thus, in this frame, the need for new antifungal agents is pressing to address the high mortality risk of IFIs.

In the last decades, we reported the discovery of a new class of non-azole antifungal agents endowed with an amidinourea macrocyclic scaffold bearing a guanidino tail. The hit compound of the series **BM1** (Figure 1) showed antifungal activity with minimum inhibitory concentration (MIC$_{50}$) values ranging from 1.25 to 20 µg/mL against several *Candida* spp. strains [19–21]. Moreover*,* it displayed an interesting in vitro and in vivo ADMET profile, even if a limited passive diffusion was highlighted in the previously reported parallel artificial permeability assay (PAMPA) [22].

A small library of derivatives was designed by modifying both the macrocyclic core and the lateral guanidino tail. In particular, the 13-membered macrocyclic portion was enlarged up to 15 carbon atoms and an *O*-phenyl group was fused with it, resulting in a remarkable inhibitory activity against representative *Candida* spp. strains, including some drug-resistant clinical isolates [19–21]. Compound **1**

(Figure 1) emerged as a good candidate for further studies, exhibiting an enhanced activity against all the tested *Candida* strains (MIC$_{90}$ values ranging from 1 to 40 µg/mL) and a more lipophilic macrocyclic scaffold due to the introduction of the *O*-phenyl group. Indeed, this chemical modification was expected to favor the establishment of additional interactions with putative targets through π-stacking and enhance the compound membrane permeability [20].

As regards the MoA of the amidinoureas class, it is still under investigation, however, in-depth studies seem to confirm an intracellular accumulation of these derivatives [21] and specific interaction with cell structures such as receptors or enzymes, as found through the previously described in silico target fishing protocol [23]. However, what we expect for amidinoureas is an innovative MoA, not shared with current antifungals, since suggested by the notable activity profile found in drug-resistant fungal strains, especially those overexpressing CDR efflux pumps [21].

In order to further explore the chemical space of the macrocyclic core, derivatives with an additional phenyl group were designed. In particular, we synthesized **2a**, characterized by a 15-membered macrocycle in which the additional phenyl ring is fused with the macrocycle in *ortho*-position and **2g** in which it is in *meta*-position, generating a 16-membered ring (Figure 1). Then, **2b–f** (Figure 1), surrounded by some representative electron-withdrawing and electron-donating groups**,** were prepared to gain an understanding of how they could affect the antifungal activity. Also, PAMPA experiments of compounds **1** and **2a–f** were performed to assess the impact of their larger core on membrane permeability, since clogP values are increased with respect to **BM1**, as calculated by SwissADME tool [24] (data not shown).

Results and discussion

Chemistry

The previously published synthetic approach [20] was adapted and optimized to prepare compounds **2a–g**. The synthesis of compounds **2a–f** and **2g** followed the same reaction steps by using different constitutional isomers as key intermediates: the *o*-vinylated derivatives **6a–f** (Scheme 1) and the *m*-vinylated one **6g** (Scheme 2).

The preparation of compounds **6a–f** started from the appropriately substituted 2-iodobenzoic acids (**a–f**) that were first reduced to benzyl alcohols **3a–f**. Then, the hydroxy group of **3a–f** was converted into a better leaving group, furnishing chlorides **4a–f**. The reaction was carried out in mild conditions with tosyl chloride, dimethylaminopyridine, and triethylamine (TEA) due to the co-presence of the more reactive iodine atom in the starting materials **3a–f** [25]. Then, **4a–f** were reacted with salicylaldehyde to furnish the

phenyl ethers **5a–f**. Finally, the palladium–catalyzed coupling with a vinyl stannane led to derivatives **6a–f** according to Stille conditions. Aldehydes **6a–f** were first converted into aldoximes **7a–f** and then reduced to benzyl amines **8a–f** via zinc-mediated hydrogenation. Derivatives **9a-f** were finally achieved by guanylating the primary amine moiety with *N,N'*-Di-Boc-1*H*-pyrazole-1-carboxamidine [26, 27]. The primary amine belonging to the previously described linker **10** [20] was reacted with the diBoc-guanidino moiety of **9a–f**, furnishing tert-butoxycarbonyl (Boc)-protected amidinoureas **11a–f** [28]. The latter compounds were endowed with two olefin groups, used as substrates for a ring-closing metathesis. To obtain macrocycles **12a–f**, the second generation Grubb's catalyst was added to a very diluted degassed CH$_2$Cl$_2$ solution of **11a–f**. A palladium-catalyzed hydrogenation led to the simultaneous removal of carboxybenzyl (Cbz) protecting group and olefin reduction, affording free amino functions that were subsequently guanylated by the *N*-crotyl-guanylating agent [19] to yield derivatives **13a–f**. In the end, final compounds **2a–f** were obtained as trifluoroacetate salts after Boc-cleavage.

Instead, the *meta*-vinylated intermediate **6g** was synthesized through Wittig reaction from *m*-xylylene dibromide in only three steps (as summarized in Scheme 2) and followed the above-mentioned synthetic route employed for the isomers **6a–f**. The whole synthetic pathway along with the intermediates procedures and characterizations were fully reported in Scheme S 1 and in *Supporting Information*.

Biological evaluation

The antifungal activity of the synthesized compounds **2a–g** was evaluated by determining MIC$_{90}$ against more than 100 strains belonging to 8 *Candida* spp. (*C. albicans, C. guilliermondii, C. crusei, C. parapsilosis, C. tropicalis, C. kefyr, C. glabrata,* and *C. lipolytica*) and 15 strains of *Cryptococcus neoformans* isolated from oral, vaginal, anorectal, urine, stool, blood, central venous catheter, and respiratory tract specimen with each strain representing a single isolate from a patient (Table 1).

All the derivatives show improved antifungal activity against almost all the tested strains, except the 16-membered macrocycle **2g** with respect to the hit compound **1** (Table 1). The introduction of a second phenyl group in the 15-membered macrocycle proved to significantly enhance the antifungal activity, as evident for compound **2a** which showed lower MIC values with respect to the correspondent mono-phenyl derivative **1** against *C. albicans, C. kefyr, C. parapsilosis,* and *C. guilliermondii*. On the other hand, a complete loss of activity against *C. lipolytica* was noticed for **2a** (Table 1). The functionalization of the new phenyl ring with one halogen atom, such as fluorine (**2b–c**) and chlorine
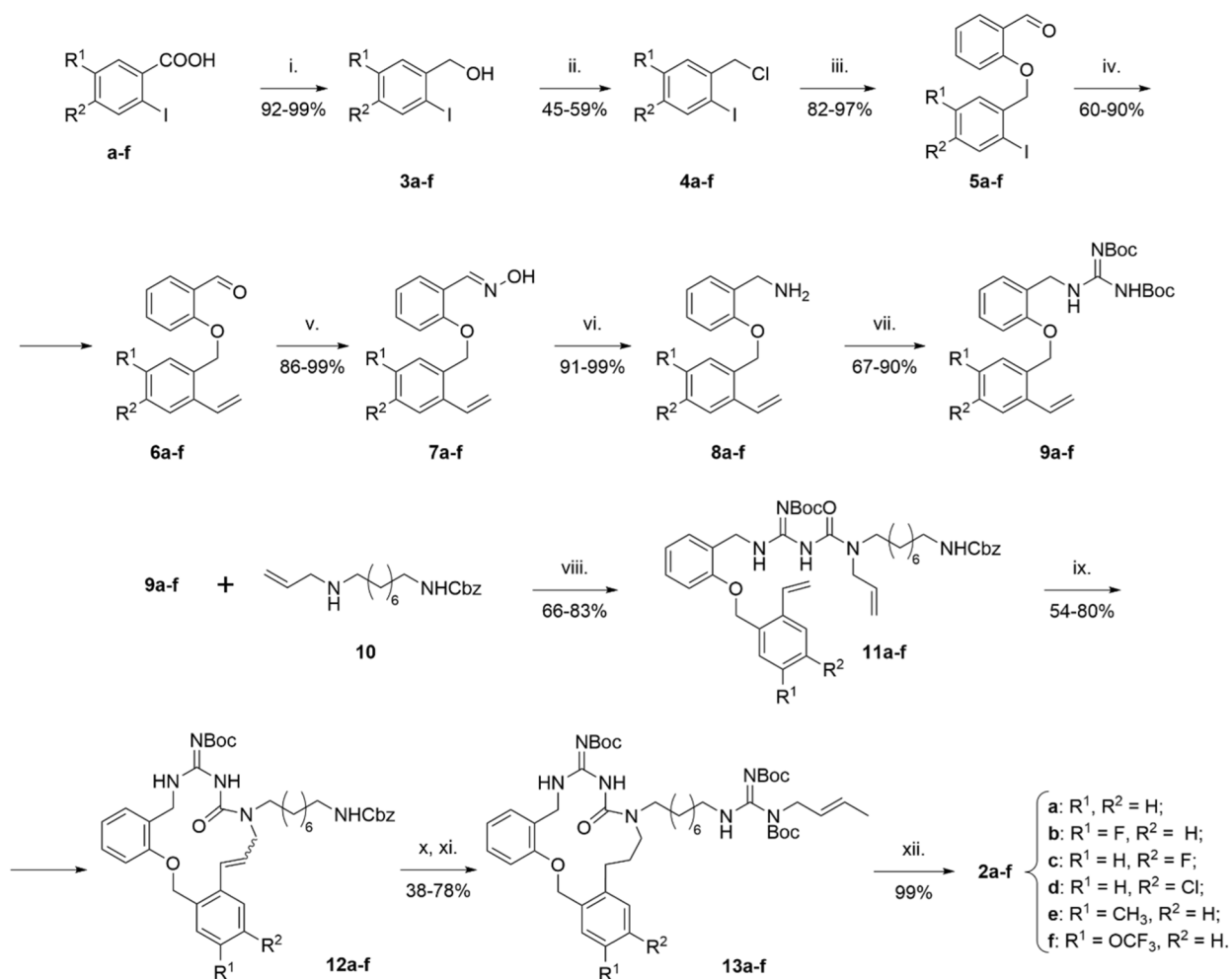
Reagents and conditions: (i.) BH₃-Me₂S, dry THF, 0 °C-r.t., 12 h, N₂; (ii.) tosyl chloride, DMAP, dry TEA, dry CH₂Cl₂, 0 °Cr. t., 16 h, N₂; (iii.) salicylaldehyde, K₂CO₃, NaI, CH₃CN, reflux, 16 h; (ii.) tributyl(vinyl)tin, Pd(OAc)₂, PPh₃, dry THF, reflux, 16 h, N₂; (v.) NH₂OH*HCl, pyridine, EtOH, reflux, 3 h; (vi.) Zn dust, 2N HCl, THF, reflux, 4 h; (vii.) *N,N'*-Di-Boc-1*H*-pyrazole-1-carboxamidine, DIPEA, THF, r. t., 16 h; (viii.) dry TEA, dry THF, reflux, 16 h, N₂; (ix.) 2ₙd gen. Grubb's catalyst, degassed dry CH₂Cl₂, reflux, 16 h, N₂; (x.) H₂, 1 atm, Pd/C 10%, cat. glacial AcOH, *i*-PrOH, r. t., 4 h; (xi.) *N,N'*-Di-Boc-*N*-crotyl-1*H*-pyrazole-1-carboxamidine, dry DIPEA, dry THF, reflux, 12 h; (xii.) TFA, CH₂Cl₂, r. t., 12 h.

Scheme 1 Synthesis of final compounds **2a–f**

Reagents and conditions are reported in *Supporting Information*.
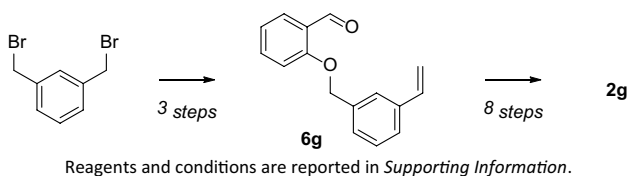
Scheme 2 Synthesis of final compound **2f**. Reagents and conditions are reported in *Supporting Information*

(**2d**), resulted in a better activity profile against some *Candida* strains. In fact, the halogenated derivatives **2b–d** exert a strong antifungal activity against *C. glabrata* with MIC

values twofold–fourfold lower than **1** and *C. guilliermondii*, *C. krusei*, and *C. kefyr* (3.12–1.56 μg/mL) and comparable activities to compound **1** toward *C. albicans*, *C. tropicalis*, and *C. parapsilosis* (Table 1).

Moreover, the substitutions in C4 and C5 of the second phenyl ring were found to impact similarly the biological activity, as highlighted by the same activity profile of the fluoro-isomers **2b** and **2c**. The best compound in terms of activity, **2d**, is less active against *C. lipolytica* than the fluorine derivatives **2b–c** (Table 1). Also, compounds bearing methyl (**2e**) and trifluoromethoxy (**2f**) substituents resulted overall active although less strong than halogenated

Table 1 MICs of derivatives library (**2a–g**) against representative *Candida* spp. and *C. neoformans* strains

Fungal strains	Antifungal activity, MIC$_{90}$ [µg/mL][a]									
	F	BM1[b]	1	2a	2b	2c	2d	2e	2f	2 g
C. albicans (22)	2	2.5	3.12	1	3.12	3.12	3.12	4	2	64
C. guilliermondii (10)	4	n.d	12.5	4	3.12	3.12	1.56	2	2	128
C. krusei (13)	256	5	6.25	8	3.12	3.12	1.56	2	4	64
C. parapsilosis (24)	0.5	5	3.12	1	3.12	3.12	3.12	16	16	64
C. tropicalis (11)	2	1.25	1.56	8	1.56	1.56	1.56	4	4	64
C. kefyr (10)	1	n.d	6.25	2	3.12	3.12	1.56	4	4	32
C. glabrata (26)	16	20	25	16	12.5	12.5	6.25	16	16	512
C. lipolytica (10)	n.d	n.d	25	256	6.25	6.25	12.5	4	4	n.a
C. neoformans (15)	2	n.d	6.25	n.d	3.12	3.12	3.12	4	4	n.d

[a]MICs are expressed in µg/mL as the average values calculated from experiments performed at least in triplicate and determined at 24 h both visually and spectrophotometrically. MIC$_{50}$ = Minimum inhibitory concentration required to inhibit the growth of 50% of organisms. MIC$_{90}$ = Minimum inhibitory concentration required to inhibit the growth of 90% of organisms. The number of tested strains per species is reported in parentheses. Fluconazole (F) and **BM1** are reported as reference control and reference compound, respectively

n.d.: not determined; n.a.: not active, no activity observed till compound concentration of 256 µg/mL

[b]MIC$_{50}$ values for **BM1** were already reported for some *Candida* species [20]

compounds **2b–d** (Table 1). In the end, derivative **2g**, characterized by a 16-membered ring, showed a dramatic loss of activity against all tested species, suggesting the key role of the macrocyclic size for biological activity. These data could confirm our hypothesis of a proteic target since tiny chemical modifications in the structure led to a total or partial loss of antifungal activity (Table 1).

In summary, 15-membered derivatives **2a–e** were found more active than the hit compound **1** against most of the fungal strains and, remarkably, active against strains not susceptible to fluconazole, *C. glabrata,* and *C. krusei.* As mentioned above*,* infections from *C. glabrata* are representing a serious threat since it is one of the most resistant fungal species, together with *C. auris*, to the azole drug-based treatments. Moreover, halogenated derivatives **2b–d** were highlighted as the most active compound of the series, showing also an inhibitory activity against *C. neoformans,* the pathogenic fungi responsible for fatal meningitis, comparable to that of fluconazole (Table 1).

Cytotoxicity on human fibroblasts

To evaluate the selectivity of the series, the cytotoxicity profile was assessed by determining the CC$_{50}$ value on Normal Human Dermal Fibroblast (FIBRO) cell line through the MTT assay. Compounds **2a**, **2b**, and **2d** were selected as the most interesting representatives of the library in terms of antifungal activity. As shown in Table 2, after 24 h, **2a** and **2b** were found to be not cytotoxic at high concentrations (CC$_{50}$ > 100 µg/mL), while **2d** a lower CC$_{50}$ (38.50 µg/mL),

still maintaining a good selectivity index (> 12) for almost all the tested strains.

PAMPA experiments

PAMPA was performed to evaluate if the introduction of an additional phenyl ring into the macrocyclic portion could be useful to gain an enhancement in the membrane permeability via passive diffusion. Thus, compounds **2a**, **2b**, and **2d** were selected as representatives of the new series, and the experiment was conducted also on compound **1** to make a comparison among the apparent permeability (P_{app}) values determined for the aliphatic macrocycle of **BM1**, the *O*-phenyl-fused macrocycle of **1**, and the tricycle core of **2**. All the tested diphenyl derivatives and **1** showed very low P_{app} values (Table 3) close to that reported for **BM1**,[22] resulting in scarce permeability, and were highly retained from the bilayer, with approximatively 50% of membrane

Table 2 In vitro cytotoxicity results on FIBRO cells for derivatives **2a**, **2b**, and **2d**

Cpd	CC$_{50}$ on FIBRO cell line [µg/mL ± S.D.]	
	24 h	48 h
2a	> 100	36.17 ± 1.86
2b	> 100	24.86 ± 1.07
2d	38.50 ± 2.18	25.44 ± 1.67

CC$_{50}$ values were determined after 24 and 48 h of incubation in FIBRO cell line. Data are reported as means ± standard deviation (S.D.) of three independent experiments, each done in triplicate

Table 3 PAMPA results for tested compounds

Cpd	Papp [10^{-6} cm/sec]	Membrane retention (%)
1	< 0.01	50.8
2a	< 0.01	55.3
2b	< 0.01	50.6
2d	< 0.01	52.1
Caffeine	1.84	3.2
Chloramphenicol	0.30	26.3

Experiments were performed in duplicate. LC-UV–MS method is described in Experimental section. Caffeine and chloramphenicol are reported as reference compounds

retention percentage. Although the chemical modification led to an increase in lipophilicity, it was not able to affect the passive absorption of these derivatives, as hypothesized. However, the high membrane retention of this class of compounds could be correlated to additional MoAs involving membranes directly or membrane proteins or transporters, as previously demonstrated [21].

Conclusion

Fungal infections represent one of the global healthy treats to date. Among compounds endowed with antifungal activity, macrocycle amidinoureas emerged for their innovative structure and their potent activity toward most *Candida* species including some resistant clinical isolates.

In this study, we investigated the insertion of a second ring into the macrocycle core of a previously described derivative **1**, by synthesizing two isomers, compounds **2a** and **2b**, endowed with a 15- and 16-membered cycle, respectively. The chemical modification led to a slightly better biological profile for **2a** and a complete loss of activity for **2f**. Also, we functionalized the phenyl ring with some representative electron-withdrawing and donating groups, such as halogen atoms, methyl, and trifluoromethoxy groups. The synthesized derivatives showed promising antifungal activity against a panel of *Candida* spp. and *C. neoformans* microorganisms that was found overall stronger than hit compound **BM1** and fluconazole. Remarkably, **2b-d** emerged as the best derivatives in terms of antifungal activity toward *C. glabrata, C. krusei, and C. kefyr,* commonly resistant to most of the current treatments and not susceptible to the azole class. We could hypothesize a possible interaction with a specific pharmacological target, such as an enzyme or receptor since tiny modifications in the chemical structure resulted in a significant change in the biological activity. However, in-depth investigation of the MoA of macrocyclic amidinoureas is still ongoing.

Furthermore, three representatives of the series, compounds **2a**, **2b**, and **2d**, were found low cytotoxic at high concentrations in MTT assays, resulting in a good selectivity index. Also, we checked these compounds for their passive permeability through PAMPA experiments. Although more lipophilic (as calculated by means of SwissADME tool)[24] than hit compound **1**, they showed low passive adsorption comparable to that of compound **1**.

In summary, the series described herein was found to exert an interesting antifungal activity, proving the impact of the insertion of the second phenyl ring into the macrocyclic scaffold in the biological profile. These results highlight this tricyclic core of the macrocyclic amidinoureas a putative starting point for the development of a new class of antifungal agents.

Experimental section

Chemistry

General Chemistry All commercially available chemicals and solvents were used as purchased. CH_2Cl_2 was dried over calcium hydride and tetrahydrofuran (THF) was dried over sodium and benzophenone before use. Degassed dry CH_2Cl_2 was prepared from freshly dried CH_2Cl_2 via three or more freeze–pump–thaw cycles. Dry DIPEA was purchased from Merck. Dry TEA was dried over KOH and distilled under nitrogen atmosphere. Anhydrous reactions were performed into flame-dried glassware after three cycles of vacuum/ dry nitrogen and were run under a positive pressure of dry nitrogen. Chromatographic separations were performed on columns packed with silica gel (230–400 mesh, for flash technique). TLCs were visualized under UV light and stained with ninhydrin, bromocresol green, or basic permanganate stains. ^{1}H NMR and ^{13}C NMR were recorded on a Bruker Avance 400 spectrometer at 400 MHz and 100 MHz, respectively. Spectra are reported in parts per million (δ scale) and internally referenced to the CDCl$_3$ and CD$_3$OD signal, respectively at δ 7.26 and 3.31 ppm. Chemical shifts for carbon are reported in parts per million (δ scale) and referenced to the carbon resonances of the solvent (CDCl$_3$ at δ 77.0 and CD$_3$OD at δ 49.0 ppm). Data are shown as following: chemical shift, multiplicity (s = singlet, d = doublet, t = triplet, q = quartet, qi = quintet, m = multiplet and/or multiplet resonances, bs = broad singlet), coupling constants (*J*) in Hertz (Hz), and integration. Mass spectra (LCMS (ESI)) were acquired using an Agilent 1100 LC-MSD VL system (G1946C) by direct injection with a 0.4 mL/min flow rate using a binary solvent system of 95/5 MeOH/H$_2$O. UV detection was monitored at 221 or 254 nm. Mass spectra were acquired in positive or negative mode scanning over

the mass range 100–1500 m/z, using a variable fragmentor voltage of 0–70 V.

Determination of purity The purity of final products (≥ 95%) was assessed by LC-UV–MS analysis using the protocol reported [29].

Synthetic procedures and characterizations of compound 2a and its intermediates

(2-iodophenyl)methanol (3a) To a stirred suspension of 2-iodobenzoic acid (3.00 g, 12.09 mmol) in dry THF (40 mL), borane dimethyl sulfide complex (3.44 mL, 36.29 mmol) was added dropwise under N_2 atmosphere at 0 °C. Then, the reaction mixture was allowed to gently warm at r.t. and stirred for 12 h. Water and K_2CO_3 were carefully added and the mixture was stirred for additional 30 min. Then, the mixture was extracted with AcOEt and washed twice with 1 N NaOH and then with brine. The organic layer was dried over anhydrous Na_2SO_4, filtered, and evaporated *in vacuo* to give pure 2-iodobenzyl alcohol **3a** as a white solid. **Yield**: 98%. **^{1}H-NMR** (400 MHz, CDCl$_3$) δ ppm 7.80 (d, $J = 8.0$ Hz, 1H), 7.43 (d, $J = 7.6$ Hz, 1H), 7.35 (t, $J = 7.2$ Hz, 1H), 6.98 (t, $J = 8.0$ Hz, 1H), 4.65 (d, $J = 5.6$ Hz, 2H), 2.49 (t, $J = 6.0$ Hz, 1H). **^{13}C-NMR** (100 MHz, CDCl$_3$) δ ppm 142.5, 139.1, 129.2, 128.4, 128.3, 97.3, 59.8.

1-(chloromethyl)-2-iodobenzene (4a) To a stirred solution of **3a** (2.78 g, 11.88 mmol) in dry CH$_2$Cl$_2$ (80 mL), freshly distilled dry TEA (1.66 mL, 11.88 mmol) and DMAP (1.74 g, 14.26 mmol) were added under N_2 atmosphere at 0 °C. Then, *p*-toluenesulfonyl chloride (4.07 g, 21.38 mmol) was added portionwise and the reaction mixture was stirred for additional 30 min at 0 °C, then at r.t. for 16 h. The solvent was removed by evaporation *in vacuo* and the crude was purified by flash chromatography on silica gel, eluting with hexane to give compound **4a**. **Yield**: 56%. **^{1}H-NMR** (400 MHz, CDCl$_3$) δ ppm 7.85 (d, $J = 7.6$ Hz, 1H), 7.47 (d, $J = 8$ Hz, 1H), 7.34 (t, $J = 7.2$ Hz, 1H), 6.99 (d, $J = 8$ Hz, 1H), 4.66 (s, 2H). **^{13}C-NMR** (100 MHz, CDCl$_3$) δ ppm 139.8, 135.6, 129.7, 129.3, 126.7, 96.8, 44.2.

2-[(2-iodophenyl)methoxy]benzaldehyde (5a) To a stirred solution of salicylaldehyde (0.50 mL, 4.69 mmol) in CH$_3$CN (10 mL), K_2CO_3 (710.0 mg, 5.16 mmol), NaI (0.18 g, 1.17 mmol), and **4a** (1.30 g, 5.16 mmol) were added and the reaction mixture was stirred at reflux for 16 h. After evaporation *in vacuo*, the residue was dissolved in AcOEt, 1 N NaOH was added, and the mixture was stirred at r.t. for additional 10 min. Then, the mixture was extracted with AcOEt three times, and the combined organic layers were washed with brine, dried over anhydrous Na_2SO_4, filtered, and evaporated *in vacuo* to give **5a**. **Yield**: 92%. **^{1}H-NMR** (400 MHz, CDCl$_3$) δ ppm 10.58 (s, 1H), 7.87 (t, $J = 7.6$ Hz, 1H), 7.56 (t, $J = 7.6$ Hz, 2H), 7.50 (m, 1H), 7.38 (t, $J = 7.2$ Hz, 2H), 7.05 (m, 2H), 5.16 (s, 2H). **^{13}C-NMR** (100 MHz, CDCl$_3$) δ

ppm 189.4, 160.8, 142.2, 139.5, 135.9, 129.6, 129.2, 128.6, 128.2, 125.3, 121.1, 113.0, 92.9, 67.9.

2-[(2-ethenylphenyl)methoxy]benzaldehyde (6a) To a stirred solution of iododerivative **5a** (1.11 g, 3.28 mmol) in dry THF (46 mL), palladium acetate (73.0 mg, 0.33 mmol) and triphenylphosphine (172.0 mg, 0.66 mmol) were added under N_2 atmosphere. Then, tributyl(vinyl)tin (1,13 mL, 3.93 mmol) was added dropwise and the reaction mixture was stirred at reflux for 16 h. After cooling, the mixture was filtered through a plug of celite, and the filtrate was evaporated *in vacuo*. The residue was diluted with AcOEt, washed with NaHCO$_3$ss and brine. Then, it was dried over anhydrous Na_2SO_4, filtered, and evaporated *in vacuo*. The crude was purified by flash chromatography on silica gel, eluting with hexane/AcOEt 9:1. **Yield**: 90%. **^{1}H-NMR** (400 MHz, CDCl$_3$) δ ppm 10.47 (s, 1H), 7.85 (d, $J = 7.7$ Hz, 1H), 7.55 (m, 2H), 7.42 (d, $J = 6.8$ Hz, 1H), 7.36 (t, $J = 7.2$ Hz, 1H), 7.30 (d, $J = 8.0$ Hz, 1H), 7.04 (m, 2H), 6.99 (dd, $J = 17.2$ Hz, 11.2 Hz, 1H), 5.70 (d, $J = 18.0$ Hz, 1H), 5.34 (d, $J = 10.8$ Hz, 1H), 5.22 (s, 2H). **^{13}C-NMR** (100 MHz, CDCl$_3$) δ ppm 189.6, 160.9, 137.2, 135.8, 133.6, 128.8, 128.3, 127.9, 126.2, 125.3, 121.0, 117.0, 113.0, 77.1, 76.8, 68.8.

Aldoxime derivative (7a) To a stirred solution of benzaldehyde **7a** (334.0 mg, 1.84 mmol) in EtOH (25 mL), pyridine (180 μL, 2.21 mmol) and hydroxylamine hydrochloride (320.0 mg, 4.6 mmol) were added. The mixture was stirred at reflux for 3 h. After cooling, the mixture was evaporated *in vacuo* and the residue was dissolved in AcOEt, washed with brine twice, dried over anhydrous Na_2SO_4, filtered, and evaporated *in vacuo*. **Yield**: 96%. **^{1}H-NMR** (400 MHz, CDCl$_3$) δ ppm 8.52 (s, 1H), 8.31 (bs, 1H), 7.75 (d, $J = 8.0$ Hz, 1H), 7.55 (d, $J = 7.6$ Hz, 1H), 7.40 (m, 1H), 7.34 (m, 3H), 6.95 (m, 3H), 5.69 (d, $J = 17.6$ Hz, 1H), 5.34 (d, $J = 10.8$ Hz, 1H), 5.14 (s, 2H). **^{13}C-NMR** (100 MHz, CDCl$_3$) δ ppm 163.5 156.6, 146.3, 137.1, 133.6, 133.1, 131.2, 128.9, 128.6, 127.8, 126.6, 126.1, 121.2, 116.9, 112.5, 68.4. **LCMS (ESI)** m/z = 276.0 [M + Na]$^+$, 254.0 [M + H]$^+$.

Benzylamino derivative (8a) To a stirred solution of aldoxime **7a** (251.0 mg, 0.99 mmol) in THF (12 mL), zinc dust (650.0 mg, 9.89 mmol) and 2 N HCl (5 mL) were added, and the reaction mixture was stirred at reflux for 4 h. After cooling, the mixture was filtered on a plug of celite, and the filtrate was evaporated *in vacuo*. The residue was dissolved in AcOEt and extracted with 3 N HCl three times. Then, the aqueous phase was basified with K_2CO_3 and extracted with CH$_2$Cl$_2$ three times. The combined organic layers were dried over anhydrous Na_2SO_4, filtered, and evaporated *in vacuo*. Compound **8a** was obtained without any further purification. **Yield**: 99%. **^{1}H-NMR** (400 MHz, CD$_3$OD) δ ppm 7.56 (d, $J = 7.7$ Hz, 1H), 7.42 (d, $J = 7.4$ Hz, 1H), 7.34 (d, $J = 7.5$ Hz, 1H), 7.29 (d, $J = 7.3$ Hz, 1H), 7.23 (d, $J = 7.1$ Hz, 2H), 7.46 (m, 3H), 5.70 (d, $J = 17.4$ Hz, 1H), 5.33 (d, $J = 11.0$ Hz, 1H), 5.12

(s, 2H), 3.81 (s, 2H), 1.62 (bs, 2H). **13C-NMR** (100 MHz, CD$_3$OD) δ ppm 156.4, 137.0, 133.8, 133.7, 131.8, 129.3, 129.2, 128.9, 128.8, 128.5, 128.3, 128.1, 127.9, 126.0, 120.9, 116.6, 111.4, 67.5, 42.1. **LCMS (ESI)** m/z = 262.1 [M + Na]$^+$, 240.1 [M + H]$^+$.

DiBoc-guanidino derivative (9a) To a stirred solution of primary amine **8a** (251.0 mg, 1.05 mmol) in THF (10 mL), *N,N′*-Di-Boc-1*H*-pyrazole-1-carboxamidine (420.2 mg, 1.36 mmol) and DIPEA (90 µL, 0.52 mmol) were added. The reaction mixture was stirred at r.t. for 16 h. After cooling, AcOEt was added, and the mixture was washed with water and brine. After drying over anhydrous Na$_2$SO$_4$, the mixture was filtered and evaporated *in vacuo*. The crude residue was purified by flash chromatography on silica gel, eluting with hexane/AcOEt 9:1 to give the pure compound **9a**. **Yield**: 78%. **1H-NMR** (400 MHz, CDCl$_3$) δ ppm 11.47 (s, 1H), 8.67 (s, 1H), 7.52 (d, J = 7.5 Hz, 1H), 7.43 (d, J = 7.3 Hz, 1H), 7.31 (t, J = 7.2 Hz, 2H), 7.25 (m, 2H), 6.95 (m, 3H), 5.66 (d, J = 17.4 Hz, 1H), 5.33 (d, J = 11.1 Hz, 1H), 5.15 (s, 2H), 4.63 (d, J = 5.6 Hz, 2H), 1.49 (s, 9H), 1.44 (s, 9H). **13C-NMR** (100 MHz, CDCl$_3$) δ ppm 163.6, 156.7, 156.3, 156.0, 152.9, 136.8, 133.7, 129.8, 128.9, 128.7, 128.2, 127.7, 126.0, 120.9, 116.7, 111.6, 82.7, 79.0, 68.1, 40.6, 28.3, 28.0. **LCMS (ESI)** m/z = 504.1 [M + Na]$^+$, 482.1 [M + H]$^+$.

Boc-amidinourea derivative (11a) To a stirred solution of **9a** (246.1 mg, 0.51 mmol) in dry THF (10 mL), a solution of linker **10** (*N*-(8-(allylamino)octyl)-2-phenylacetamide (261.0 mg, 0.82 mmol) in dry THF (5 mL) and freshly distilled dry TEA (70 µL, 0.51 mmol) were added dropwise under N$_2$ atmosphere. The reaction mixture was stirred at reflux for 16 h. After cooling, AcOEt was added, and the mixture was washed with water and brine. After drying over anhydrous Na$_2$SO$_4$, the mixture was filtered and evaporated *in vacuo*. The crude residue was purified by flash chromatography on silica gel, eluting with hexane/AcOEt 8:2 to give pure compound **11a**. **Yield**: 73%. **1H-NMR** (400 MHz, CDCl$_3$) δ ppm 12.28 (s, 1H), 8.41 (s, 1H), 7.52 (d, J = 7.5 Hz, 1H), 7.44 (d, J = 7.4 Hz, 1H), 7.35 (m, 5H), 7.32 (d, J = 6.9 Hz, 1H), 7.29 (d, J = 7.3 Hz, 2H), 7.25 (m, 1H), 7.02 (m, 1H), 6.94 (d, J = 9.7 Hz, 2H), 5.77 (m, 1H), 5.66 (d, J = 16.4 Hz, 1H), 5.32 (d, J = 10.8 Hz, 1H), 5.15 (s, 2H), 5.09 (m, 4H), 5.01 (d, J = 9.9 Hz, 1H), 4.55 (dd, J = 14.8 Hz, 6.0 Hz, 2H), 4.05 (d, J = 5.3 Hz, 1H), 3.89 (d, J = 5.3 Hz, 1H), 3.36 (t, J = 7.6 Hz, 1H), 3.21 (t, J = 8.0 Hz, 1H), 3.14 (m, 2H), 1.51 (m, 4H), 1.42 (s, 9H), 1.21 (m, 8H). **13C-NMR** (100 MHz, CDCl$_3$) δ ppm 163.7, 156.5, 154.1, 153.9, 153.3, 135.3, 134.7, 133.7, 129.3, 129.0, 128.7, 128.6, 128.4, 128.4, 128.0, 127.8, 126.8, 126.0, 120.7, 116.7, 115.5, 111.5, 81.9, 68.1, 66.5, 50.5, 48.5, 47.5, 45.7, 41.0, 40.1, 29.8, 29.4, 29.2, 28.5, 28.0, 27, 26.9, 26.6. **LCMS (ESI)** m/z = 748.9 [M + Na]$^+$, 726.9 [M + H]$^+$.

Unsaturated macrocyclic amidinourea (12a) To a stirred solution of amidinourea derivative **9a** (247.1 mg, 0.34 mmol) in freshly degassed dry CH$_2$Cl$_2$ (170 mL, 2 mM solution), a solution of 2nd generation Grubb's catalyst (58.0 mg, 0.2 mmol) in freshly degassed dry CH$_2$Cl$_2$ (2 mL) was added dropwise under N$_2$ atmosphere. The reaction mixture was stirred at reflux for 16 h. After cooling, the mixture was evaporated *in vacuo*. The crude residue was purified by flash chromatography on silica gel, eluting with hexane/AcOEt 85:15 to give macrocycle **12a**. **Yield**: 75%. **1H-NMR** (400 MHz, CDCl$_3$) δ ppm 12.27 (bs, 1H), 8.40 (m, 1H), 7.58 (d, J = 8.0 Hz, 1H), 7.32 (m, 6H), 7.23 (m, 3H), 6.98 (m, 3H), 6.58 (d, J = 15.6 Hz, 1H), 6.16 (dt, J = 15.6 Hz, 5.2 Hz, 1H), 5.15 (s, 2H), 5.08 (s, 2H), 4.69 (bs, 1H), 4.61 (d, J = 6.4 Hz, 2H), 3.92 (d, J = 5.2 Hz, 2H), 3.35 (t, J = 7.6 Hz, 2H), 3.16 (m, 2H), 1.57 (s, 4H), 1.46 (m, 9H), 1.23 (s, 8H). **13C-NMR** (100 MHz, CDCl$_3$) δ ppm 163.7, 155.3, 154.2, 153.6, 138.1, 137.8, 136.9, 129.6, 129.4, 129.1, 128.8, 128.7, 128.3, 126.5, 122.9, 118.6, 99.9, 82.2, 72.2, 66.5, 45.1, 44.1, 43.4, 40.9, 31.1, 29.3, 29.2, 28.5, 27.3. **LCMS (ESI)** m/z = 698.2 [M + H]$^+$.

DiBoc-guanidino macrocyclic amidinourea (13a) To a stirred solution of **10a** (180.2 mg, 0.17 mmol) in isopropanol (19 mL), Pd/C 10% (32.0 mg, 0.03 mmol) and a few drops of glacial AcOH were added. The reaction mixture was subject to three cycles of *vacuo* followed by a flush of H$_2$ before being stirred under H$_2$ (1 atm) for 4 h. Then, the mixture was filtered through a plug of celite, and the filtrate was evaporated *in vacuo*. The crude product was used directly in the next step without any further purification. **LCMS (ESI)** m/z = 566.3 [M + H]$^+$. To a stirred solution of the crude in dry THF (4.5 mL), a solution of the crotyl guanylating agent (*N,N′*-Di-Boc-(E)-*N*-crotyl-1*H*-pyrazole-1-carboximidamide, 60.0 mg, 0.17 mmol) in dry THF (2.8 mL) and dry DIPEA (89 µL, 0.51 mmol) were subsequently added under N$_2$ atmosphere. The reaction mixture was stirred at reflux for 12 h. After cooling, the mixture was evaporated *in vacuo* and the residue was dissolved in AcOEt, washed with water twice and brine. After drying over anhydrous Na$_2$SO$_4$, the mixture was filtered, and evaporated *in vacuo*. The crude residue was purified by flash chromatography on silica gel, eluting with hexane/AcOEt 8:2 to give pure compound **13a**. **Yield**: 52% over two steps. **1H-NMR** (400 MHz, CDCl$_3$) δ ppm 12.20 (s, 1H), 8.54 (s, 1H), 7.37 (d, J = 7.5 Hz, 1H), 7.31 (m, 1H), 7.26 (s, 1H), 7.23 (d, J = 6.7 Hz, 1H), 7.20 (d, J = 7.5 Hz, 1H), 6.99 (d, J = 7.8 Hz, 1H), 6.95 (d, J = 7.5 Hz, 1H), 6.83 (m,1 H), 5.65 (m, 1H), 5.50 (m, 1H), 5.06 (s, 2H), 4.57 (d, J = 6.3 Hz, 2H), 4.15 (d, J = 5.4 Hz, 2H), 3.18 (m, 6H), 2.53 (m, 2H), 1.97 (m, 2H), 1.65 (d, J = 5.8 Hz, 3H), 1.48 (m, 31H), 1.29 (s, 8H). **13C-NMR** (100 MHz, CDCl$_3$) δ ppm 163.6, 156.0, 155.5, 153.6, 153.3, 142.7, 134.0, 130.7, 129.9, 129.7, 128.9, 127.7,

127.4, 126.5, 126.1 125.8, 120.6, 110.6, 82.9, 82.1, 79.1, 69.4, 60.3, 49.9, 47.3, 40.9, 38.1, 30.8, 30.2, 29.6, 29.3, 29.2, 28.9, 28.7, 28.2, 28.1, 28.0, 27.0, 26.8, 20.9, 17.1. **LCMS (ESI)** $m/z = 884.3$ [M + Na]$^+$, 862.4 [M + H]$^+$.

Guanidino macrocylic amidinourea trifluoroacetate salt (2a) To a stirred solution of **13a** (10.0 mg, 0,014 mmol) in dry CH_2Cl_2 (1.7 mL), freshly distilled TFA (300 μL, final concentration 10% v/v) was added dropwise. The reaction mixture was stirred at r.t. for 12 h. The mixture was evaporated in vacuo. Then, it was treated with toluene and methanol and evaporated in vacuo to remove TFA residue. The crude was treated with Et_2O and hexane and then decanted, and the solvents were pipetted off. This procedure was repeated several times to yield compound **2a**. **Yield**: 99%. **^{1}H-NMR** (400 MHz, CD$_3$OD) δ ppm 7.45 (d, $J = 6.9$ Hz, 1H), 7.36 (d, $J = 5.6$ Hz, 2H), 7.27 (dd, $J = 17.5$ Hz, 7.6 Hz, 1H), 7.21 (d, $J = 8.0$ Hz, 1H), 7.08 (dd, $J = 11.7$ Hz, 6.5 Hz, 1H), 7.07 (m, 1H), 6.86 (d, $J = 8.9$ Hz, 1H), 5.73 (m, 1H), 5.49 (m, 1H), 5.07 (s, 2H), 4.43 (m, 2H), 3.74 (d, $J = 5.4$ Hz, 2H), 3.39 (m, 1H), 3.28 (d, $J = 12.8$ Hz, 1H), 3.15 (t, $J = 7.1$ Hz, 2H), 2.82 (s, 1H), 2.61 (s, 1H), 2.09 (m, 1H), 1.85 (m, 1H), 1.70 (d, $J = 6.4$ Hz, 3H), 1.55 (m, 6H), 1.31 (m, 8H). **^{13}C-NMR** (100 MHz, CD$_3$OD) δ ppm 157.4, 155.0, 152.0, 131.2, 131.1, 130.8, 130.1, 129.6, 127.2, 127.0, 126.4 125.4, 124.1, 122.5, 122.0, 121.0, 117.1, 116.3, 113.4, 85.9, 79.3, 44.0, 42.5, 30.7, 30.3, 30.2, 30.0, 27.6, 17.8. **LCMS (ESI)** $m/z = 584.4$ [M + Na]$^+$, 562.3 [M + H]$^+$, 281.7 [M + 2H]$^{2+}$.

Procedures and characterizations for final compounds 2b-g and their intermediates (3-13b-g and 14–15) are reported in *Supporting Information*.

Antifungal activity testing

Yeast cells were grown in yeast peptone dextrose (YPD) medium at 37 °C for 16 h and 150 rpm orbital shaker. Cells were then sub-inoculated in fresh YPD medium and grown to an optical density of 0.3. The turbidity of the inoculum was adjusted to 0.5 McFarland and diluted 1:500 in RPMI 1640 broth, corresponding to around 2.5×10^5 CFU/mL. MICs were determined by liquid growth inhibition assays by Clinical and Laboratory Standards Institute (CLSI) guidelines, using serial dilutions of the compounds dissolved in an appropriate buffer with a final concentration ranging from 256 to 0.125 μg/mL in a 96-well flat-bottomed microtiter plate [30]. Plates were incubated at 35 °C, and MICs were visualized after 24 h as the lowest concentration of the tested compound that completely inhibited cell growth.

MTT assay

All chemicals were purchased from Euroclone (Milan, Italy). In vitro cytotoxicity on normal human dermal fibroblasts, purchased from American Type Culture Collection (ATCC) (Manassas, VA). Cells were cultured in Dulbecco's modified Eagle's medium (DMEM), supplemented with 10% fetal bovine serum (FBS), 2 mM L-glutamine, and 10,000 units/mL penicillin/streptomycin at 37 °C in a 5% CO_2 v/v atmosphere. Briefly, 5×10^3 cells/well were plated in 0.2 mL of medium/well in 96-well plates, the day after seeding, a solution of the test compound in dimethyl sulfoxide (DMSO) (0.1 to 100 μg/mL) was added and incubated for 24 and 48 h at 37 °C in 5% v/v CO_2 atmosphere. After incubation, the medium was carefully removed and each well was washed with Dulbecco's phosphate-buffered saline (PBS) twice and 150 μL of 3-(4,5-dimethylthiazol-2-yl)-2,5-diphenyltetrazolium bromide (MTT) (5 mg/mL) in Minimum Essential Medium (MEM) were added. The plates were incubated for 3 h in a 5% v/v CO_2 atmosphere. After incubation, 100 μL of isopropanol were added to each well and plates were shaken at r.t. for 30 min. The optical density was measured by a microtiter plate reader (Multiskan SkyHigh Microplate Spectrophotometer, Thermo Fisher, Italy) at 570 nm. CC_{50} values were calculated by GraphPad Prism 6.0 software using the best fitting sigmoid curve. For each compound, the determination was performed in triplicate.

PAMPA experiments

P_{app} values of the tested compounds were evaluated as previously reported.[31] Briefly, for each compound, a donor solution was prepared from a stock solution of the test compound in DMSO (1 mM) diluted with PBS (pH 7.4, 25.0 mM) to a final concentration of 500 μM. Donor wells were filled with 150 μL of the donor solution. Filters were coated with 5 μL of a 1% w/v phosphatidylcholine (L-α-phosphatidylcholine egg yolk, Type XVI-E, purchased from Merck) in dodecane solution and the lower wells were filled with 300 μL of the acceptor solution (DMSO/PBS 1:1). The sandwich plate was assembled and incubated at r.t. for 5 h under gentle agitation. After the incubation time, the sandwich was disassembled and the amount of compound in each donor and acceptor wells was measured by the LC-UV–MS protocol. For each compound, the determination was performed in three independent experiments. P_{app} and MR% values were calculated as reported [32, 33].

Determination of pan-assay interference compounds

The behavior of all the tested compounds (**2a-g**) as pan-assay interference compounds (PAINS) was examined through

prediction by the web tools SwissADME [24, 34] and false positive remover, and no alert of PAINS was recorded.

Supplementary Information

The online version contains supplementary material available at and contains the following paragraphs: Preparation of compound **2g**. Chemical procedures and characterizations for final compounds **2b-g**; ^{1}H and ^{13}C NMR spectra of some derivatives as representatives of the series.

Declarations

Conflicts of interest. The authors declare that there is no conflict of interest.

References

1. Kainz K, Bauer MA, Madeo F, Carmona-Gutierrez D (2020) Fungal infections in humans: the silent crisis. Microb. cell 7:143–145. https://doi.org/10.15698/mic2020.06.718

2. Li Y, Gao Y, Niu X et al (2020) A 5-year review of invasive fungal infection at an academic medical center. Front Cell Infect Microbiol 10:553648. https://doi.org/10.3389/fcimb.2020.553648

3. Bongomin F, Gago S, Oladele RO, Denning DW (2017) Global and multi-national prevalence of fungal diseases—estimate precision. J Fungi 3(4):57. https://doi.org/10.3390/jof3040057

4. Limper AH, Adenis A, Le T, Harrison TS (2017) Fungal infections in HIV/AIDS. Lancet Infect Dis 17:e334–e343. https://doi.org/10.1016/S1473-3099(17)30303-1

5. Höfs S, Mogavero S, Hube B (2016) Interaction of Candida albicans with host cells: virulence factors, host defense, escape strategies, and the microbiota. J Microbiol 54:149–169. https://doi.org/10.1007/s12275-016-5514-0

6. Pathakumari B, Liang G, Liu W (2020) Immune defence to invasive fungal infections: a comprehensive review. Biomed Pharmacother 130:110550. https://doi.org/10.1016/j.biopha.2020.110550

7. Cataldo MA, Tetaj N, Selleri M et al (2020) Incidence of bacterial and fungal bloodstream infections in COVID-19 patients in intensive care: an alarming "collateral effect." J Glob Antimicrob Resist 23:290–291. https://doi.org/10.1016/j.jgar.2020.10.004

8. Rawson TM, Moore LSP, Zhu N et al (2020) Bacterial and fungal coinfection in individuals with coronavirus: a rapid review to support COVID-19 antimicrobial prescribing. Clin Infect Dis 71(9):2459–2468. https://doi.org/10.1093/cid/ciaa530

9. Song G, Liang G, Liu W (2020) Fungal co-infections associated with global COVID-19 pandemic: a clinical and diagnostic perspective from China. Mycopathologia 185:599–606. https://doi.org/10.1007/s11046-020-00462-9

10. Fernández-García R, de Pablo E, Ballesteros MP, Serrano DR (2017) Unmet clinical needs in the treatment of systemic fungal infections: the role of amphotericin B and drug targeting. Int J Pharm 525:139–148. https://doi.org/10.1016/j.ijpharm.2017.04.013

11. Brown GD, Denning DW, Gow NARR et al (2012) Hidden killers: human fungal infections. Sci Transl Med 4(165):165rv13. https://doi.org/10.1126/scitranslmed.3004404

12. Seyoum E, Bitew A, Mihret A (2020) Distribution of *Candida albicans* and non-albicans *Candida* species isolated in different clinical samples and their in vitro antifungal suscetibity profile in Ethiopia. BMC Infect Dis 20:231. https://doi.org/10.1186/s12879-020-4883-5

13. Posteraro B, Sanguinetti M, Fiori B et al (2006) Caspofungin activity against clinical isolates of azole cross-resistant *Candida glabrata* overexpressing efflux pump genes. J Antimicrob Chemother 58:458–461. https://doi.org/10.1093/jac/dkl237

14. Gabaldón T, Gómez-Molero E, Bader O (2020) Molecular typing of *Candida glabrata*. Mycopathologia 185:755–764. https://doi.org/10.1007/s11046-019-00388-x

15. Perlin DS, Rautemaa-Richardson R, Alastruey-Izquierdo A (2017) The global problem of antifungal resistance: prevalence, mechanisms, and management. Lancet Infect Dis 17:e383–e392. https://doi.org/10.1016/S1473-3099(17)30316-X

16. Lin YY, Shiau S, Fang CT (2015) Risk factors for invasive *Cryptococcus neoformans* diseases: a case-control study. PLoS ONE 10(3):e0119090. https://doi.org/10.1371/journal.pone.0119090

17. Roemer T, Krysan DJ (2014) Unmet clinical needs, and new approaches. Cold Spring Harb Perspect Med 4:a019703

18. Shaw KJ, Ibrahim AS (2020) Fosmanogepix: a review of the first-in-class broad spectrum agent for the treatment of invasive fungal infections. J Fungi 6(4):239. https://doi.org/10.3390/jof6040239

19. Manetti F, Castagnolo D, Raffi F et al (2009) Synthesis of new linear guanidines and macrocyclic amidinourea derivatives endowed with high antifungal activity against *Candida* spp. and *Aspergillus* spp. J Med Chem 52(23):7376–7379. https://doi.org/10.1021/jm900760k

20. Sanguinetti M, Sanfilippo S, Castagnolo D et al (2013) Novel macrocyclic amidinoureas: potent non-azole antifungals active against wild-type and resistant Candida species. ACS Med Chem Lett 4:852–857. https://doi.org/10.1021/ml400187w

21. Deodato D, Maccari G, De Luca F et al (2016) Biological characterization and in vivo assessment of the activity of a new synthetic macrocyclic antifungal compound. J Med Chem 59:3854–3866. https://doi.org/10.1021/acs.jmedchem.6b00018

22. Orofino F, Truglio GI, Fiorucci D et al (2020) In vitro characterization, ADME analysis, and histological and toxicological evaluation of BM1, a macrocyclic amidinourea active against azole-resistant Candida strains. Int J Antimicrob Agents 55:105865. https://doi.org/10.1016/j.ijantimicag.2019.105865

23. Maccari G, Deodato D, Fiorucci D et al (2017) Design and synthesis of a novel inhibitor of *T. Viride* chitinase through an in silico target fishing protocol. Bioorg Med Chem Lett 27:3332–3336. https://doi.org/10.1016/j.bmcl.2017.06.016

24. Daina A, Michielin O, Zoete V (2017) SwissADME: a free web tool to evaluate pharmacokinetics, drug-likeness and medicinal chemistry friendliness of small molecules. Sci Rep 71(7):1–13. https://doi.org/10.1038/srep42717

25. Ding R, He Y, Wang X et al (2011) Treatment of alcohols with tosyl chloride does not always lead to the formation of tosylates. Molecules 16:5665–5673. https://doi.org/10.3390/molecules16075665

26. Pasero C, D'Agostino I, De Luca F et al (2018) Alkyl-guanidine compounds as potent broad-spectrum antibacterial agents: chemical library extension and biological characterization. J Med Chem. https://doi.org/10.1021/acs.jmedchem.8b00619

27. Zamperini C, Maccari G, Deodato D et al (2017) Identification, synthesis and biological activity of alkyl-guanidine oligomers as potent antibacterial agents. Sci Rep 7:8251. https://doi.org/10.1038/s41598-017-08749-6

28. D'Agostino I, Ardino C, Poli G, et al (2022) Antibacterial alkyl-guanidino ureas: Molecular simplification approach, searching for membrane-based MoA. Eur J Med Chem 114158. https://doi.org/10.1016/J.EJMECH.2022.114158

29. Miel H, Rault S (1998) Conversion of N, N'-bis(tert-butoxycarbonyl)guanidines to N-(N'-tert-butoxycarbonylamidino)ureas. Tetrahedron Lett 39(12):1565–1568. https://doi.org/10.1016/S0040-4039(98)00025-2

30. CLSI (2017) Reference method for broth dilution antifungal susceptibility testing of yeasts. 4st ed. CLSI guideline M27. Clinical and Laboratory Standards Institute, Wayne, PA

31. Rango E, D'Antona L, Iovenitti G et al (2021) Si113-prodrugs selectively activated by plasmin against hepatocellular and ovarian carcinoma. Eur J Med Chem 223:113653. https://doi.org/10.1016/j.ejmech.2021.113653

32. Wohnsland F, Faller B (2001) High-throughput permeability pH profile and high-throughput alkane/water log P with artificial membranes. J Med Chem 44:923–930. https://doi.org/10.1021/jm001020e

33. Sugano K, Hamada H, Machida M, Ushio H (2001) High throughput prediction of oral absorption: improvement of the composition of the lipid solution used in parallel artificial membrane permeation assay. J Biomol Screen 6:189–196. https://doi.org/10.1177/1087705710100600309

34. Baell JB, Holloway GA (2010) New substructure filters for removal of pan assay interference compounds (PAINS) from screening libraries and for their exclusion in bioassays. J Med Chem 53:2719–2740. https://doi.org/10.1021/jm901137j

Authors and Affiliations

Lorenzo J. I. Balestri[1] · Ilaria D'Agostino[1] · Enrico Rango[1] · Chiara Vagaggini[1] · Rosalba Marchitiello[2] · Melinda Mariotti[2] · Alexandru Casian[1] · Davide Deodato[1] · Giuseppina I. Truglio[1] · Francesco Orofino[1] · Maurizio Sanguinetti[2,3] · Francesca Bugli[2,3] · Lorenzo Botta[4,5] · Elena Dreassi[1]

1   Department of Biotechnology, Chemistry and Pharmacy, University of Siena, 53100 Siena, Italy

2   Dipartimento Di Scienze Biotecnologiche Di Base, Cliniche Intensivologiche E Perioperatorie, Università Cattolica del Sacro Cuore, Rome, Italy

3   Dipartimento Di Scienze Di Laboratorio E Infettivologiche, Fondazione Policlinico Universitario A. Gemelli IRCCS, Rome, Italy

4   Lead Discovery Siena S.R.L, Via Vittorio Alfieri 31, 53019 Castelnuovo Berardenga, Italy

5   Department of Ecological and Biological Sciences, University of Tuscia, Largo Università S.N.C, 01100 Viterbo, Italy